Int J Legal Med
DOI 10.1007/s00414-017-1622-6

ORIGINAL ARTICLE

# Temperature-corrected post-mortem 1.5 T MRI quantification of non-pathologic upper abdominal organs

**Nicole Schwendener[1] · Christian Jackowski[1] · Frederick Schuster[1,2] · Anders Persson[3] · Marcel J. Warntjes[3] · Wolf -Dieter Zech[1,3]**

Received: 9 December 2016 / Accepted: 2 June 2017


**Abstract**
*Objectives* The present study aimed to evaluate if simultaneous temperature-corrected T1, T2, and proton density (PD) 1.5 T post-mortem MR quantification [quantitative post-mortem magnetic resonance imaging (QPMMRI)] is feasible for characterizing and discerning non-pathologic upper abdominal organs (liver, spleen, pancreas, kidney) with regard to varying body temperatures.
*Methods* QPMMRI was performed on 80 corpses (25 females, 55 males; mean age 56.2 years, SD 17.2) prior to autopsy. Core body temperature was measured during QPMMRI. Quantitative T1, T2, and PD values were measured in the liver, pancreas, spleen, and left kidney and temperature corrected to 37 °C. Histologic examinations were conducted on each measured organ to determine non-pathologic organs. Quantitative T1, T2, and PD values of non-pathologic organs were ANOVA tested against values of other non-pathologic organ types.
*Results* Based on temperature-corrected quantitative T1, T2, and PD values, ANOVA testing verified significant differences between the non-pathologic liver, spleen, pancreas, and left kidneys.
*Conclusions* Temperature-corrected 1.5 T QPMMRI based on T1, T2, and PD values may be feasible for characterization and differentiation of the non-pathologic liver, spleen, pancreas, and kidney. The results may provide a base for future specific pathology diagnosis of upper abdominal organs in post-mortem imaging.

**Keywords** Post-mortem magnetic resonance imaging · Post-mortem MRI quantification · Abdominal organs · Relaxation times · Proton density

**Abbreviations**

| | |
|---|---|
| AUC | Area under curve |
| CV | Coefficient of variation |
| MRI | Magnetic resonance imaging |
| NP | Non-pathologic |
| PD | Proton density |
| PMMRI | Post-mortem magnetic resonance imaging |
| PMCT | Post-mortem computed tomography |
| PMI | Post-mortem interval |
| QPMMRI | Quantitative post-mortem magnetic resonance imaging |
| ROC | Receiver operator characteristic |
| ROI | Region of interest |
| SAR | Specific absorption rate |
| T | Tesla |
| T2w | T2 weighted |
| TR | Repetition time |
| TSE | Turbo spin echo |

## Introduction

In the last decade, post-mortem magnetic resonance imaging (PMMRI) has been implemented into post-mortem imaging as a useful adjunct to forensic autopsy [1–4]. Only recently

✉ Wolf -Dieter Zech
Wolf-Dieter.Zech@irm.unibe.ch

[1] Institute of Forensic Medicine, University of Bern, Buehlstrasse 20, 3012 Bern, Switzerland

[2] Department of Diagnostic, Interventional and Pediatric Radiology, University of Bern, Inselspital, Freiburgstrasse 10, CH-3010 Bern, Switzerland

[3] Center for Medical Image Science and Visualization (CMIV), University of Linköping, 58185 Linköping, Sweden

Published online: 17 June 2017

quantitative PMMRI (QPMMRI) has been introduced to post-mortem imaging [5–7]. A particular quantitative MRI sequence feasible for simultaneous quantification of T1 and T2 relaxation times as well as proton density (PD) was applied to quantify and characterize post-mortem heart and brain tissue. The results of these studies indicated that simultaneous quantification of T1, T2, and PD may be used for advanced post-mortem diagnosis of basic soft tissue pathology [8–12]. The conducted QPMMRI studies concurrently demonstrated that assessment of relaxation times for characterization of soft tissue bears two practical problems. One problem is that MR relaxation times, T1 relaxation times in particular, are dependent on body temperature. In post-mortem imaging, the temperature of scanned deceased bodies can range between 0 and 40 °C [6, 9]. Hence, if the quantitative MR values of corpses with different body temperatures are to be used for tissue characterization and comparison, body temperature has to be measured and temperature correction of quantitative values has to be performed. The second problem of QPMMRI is the dependence of MR relaxation times on magnetic field strength [13]. Currently, both 1.5 and 3 T MR machines are being used in PMMRI. Concurrently, the T1 and T2 relaxation times of one and the same tissue differ between 1.5 and 3 T applications [5, 9]. Therefore, in order to use MR relaxation time values for pathology diagnosis in routine post-mortem casework, the quantitative values of regular tissues and pathologic tissues for both 1.5 and 3 T applications need to be known first [9–11]. Moreover, it has been demonstrated that post-mortem relaxation time values differ to the known in vivo values of thoraco-abdominal organs and tissues [6, 9]. Therefore, the known in vivo values cannot be used reliably for tissue characterization in QPMMRI. So far, only regular hepatic T1 and T2 relaxation times were investigated in a 1.5 T post-mortem application [6]. The quantitative post-mortem 1.5 T values and temperature dependence of other relevant upper abdominal organs such as the pancreas, spleen, and kidney need to be determined and compared yet. As part of this basic research evaluation, the present study aimed to evaluate if simultaneous temperature-corrected T1, T2, and PD 1.5 T QPMMRI is feasible for characterizing and discerning non-pathologic upper abdominal organs (liver, spleen, pancreas, and kidney) with regard to varying body temperatures.

## Methods

### Study population

PMMRI and QPMMRI were conducted on 80 corpses (25 females, 55 males) in a prospective study between June 2013 and June 2015. Study cases were routine forensic cases in which forensic autopsies were ordered by the local authorities. The age at death ranged from 26 to 93 years (mean age 56.2 years, SD 17.2). PMMRI examinations and usage of the imaging data were approved by the local ethics committee. Post-mortem interval (PMI: time between death and PMMRI) ranged from 6 h to 2 days. Prior to PMMRI, all corpses underwent whole body post-mortem computed tomography (PMCT) scanning as part of in-house routine forensic examinations. Corpses with signs of relevant putrefaction gas formations in PMCT images were excluded from the study. Causes of death in the investigated 80 cases were myocardial infarction, acute cardiac arrest, pericardial tamponade, acute intoxication, and exsanguination.

### Magnetic resonance imaging

For PMMRI (Siemens Magnetom Symphony Tim 1.5 T; TIM body coil), corpses were wrapped in an artifact-free body bag. Subjects were examined in the supine position. Examinations included a quantification sequence as well as conventional T1-, T2-, and PD-weighted sequences. The PMMRI examination time was 1 h, of which the quantification sequence lasted 20 min. The quantification sequence used was a multi-slice turbo spin echo (TSE) sequence, where each acquisition was performed with eight different echo times at multiples of 13.5 ms (13.5–108 ms), flip angle 180° [14]. Four different saturation delay times were acquired at 100, 400, 1100, and 2400 ms, using a TR of 2500 ms. In this setup, 32 different images were acquired per slice, with different effects of T1 and T2 relaxation. Twenty slices of 4 mm thickness in cardiac short axis plane orientation were acquired with a gap of 0.3 mm. The covered scan area included the downer thoracic region and the upper abdominal region. Field of view (257 × 300 mm) was adapted to cover these body parts with a resulting in plane resolution of 0.78 mm (Matrix 384 × 330). The sequence kernel (with timings of TE, TR, and TI) was kept identical to the original neuro-application sequence [14]. T1 and T2 relaxation times and PD of upper abdominal organs and tissues were retrieved by a commercially available post-processing tool (SyMRI Autopsy®, SyntheticMR, Linköping/Sweden) [15]. The same software provided synthetic T1-, T2-, and PD-weighted images for visual support. In each case, additional conventional T1-, T2-, and PD-weighted images with a slice thickness of 3 mm and a gap of 0.3 mm were acquired. During the PMMRI scans, the corpse core body temperatures were assessed in real time with MR-compatible temperature probes (Temperature Transmitter FTX-300, Fiber Optic Temperature Probe PRB-MR1, Osensa Innovations, Canada) that were placed deep into the esophagus (probe tip situated behind the heart) before the MR examination as described in previous studies [9, 11].

### Measurement of quantitative values in QPMMRI

Quantitative T1, T2 (both in ms), and PD (as %) values were measured in synthetically calculated QPMMRI images of the liver, pancreas, spleen, and left kidney using the SyMRI Autopsy® tool at a regular radiological workstation (Fig. 1) [15]. A total of nine regions of interests (ROIs) were placed in each investigated organ in at least three different slices at the following locations: liver: left lobe, right lobe, caudate lobe; pancreas: head, body, tail; spleen: anterior extremity, mid-section, posterior extremity; left kidney cortex: upper pole, mid-section, inferior pole; and left kidney medulla: upper pole, mid-section, inferior pole. Means and standard deviations were calculated out of nine measurements for each organ in each case. The size of the rectangular ROIs was at least 5 pixels and at maximum 13 pixels in each dimension. ROIs were deliberately not placed in areas with larger blood vessels. All quantitative measurements were conducted by one observer with 7 years of experience in post-mortem magnetic resonance imaging.

### Autopsy and histologic examinations

Forensic autopsies were conducted immediately after PMMRI examinations by board-certified forensic pathologists according to the Recommendation of the Committee of Ministers to Member States of Europe on the harmonization of medicolegal autopsy rules [16]. At autopsy tissue specimens of the liver, spleen, pancreas, and kidneys were secured for routine histologic examinations (histology stain used was hematoxylin and eosin (H&E)). These tissue specimens were obtained and investigated as part of the routine post-mortem examinations that were ordered by the local authorities. Histologic examinations were conducted on each organ that was measured in QPMMRI. Histologic diagnoses were made by board-certified forensic pathologists. Only organs that appeared non-pathologic (without signs of edema, fibrosis, fatty degeneration, acute necrosis, infarction, inflammation, tumor, acute or chronic blood congestion) at histologic examinations were included into this study.

### Temperature correction of quantitative values

Body core temperatures of corpses were assessed during QPMMRI and plotted against the respective measured quantitative T1, T2, and PD values of organs. Coefficients of variations (CV) of T1, T2, and PD values for each investigated organ were calculated. CV was defined as the ratio of the standard to the mean of assessed T1, T2, and PD values and calculated for temperature-corrected and non-temperature-corrected values.

Microsoft Excel® was used to generate linear equations from T1/temperature, T2/temperature, and PD/temperature plots of non-pathologic organs. These equations were used to correct quantitative T1, T2, and PD values to a temperature of 37 °C per the following method [9–12]: in each case, measured corpse temperatures were subtracted from 37 °C (Δtemperatures). Δtemperatures were applied in the linear equations generated from quantitative value/temperature plots to gain ΔT1, ΔT2, and ΔPD. Those Δ values were summated to the uncorrected T1, T2, and PD values to gain temperature-corrected T1, T2, and PD values.

To visualize clustering and separation of temperature-corrected quantitative non-pathologic organs, mean temperature-corrected quantitative T1, T2, and PD values of the liver, spleen, pancreas, and kidney were plotted in a 3D plot using the ThreeDifyExcelGrapher add-in for Microsoft Excel®.

### Statistical analyses

SPSS® was used to perform a series of one-way Welch *F* test ANOVAs with post hoc analysis to evaluate significant differentiability of temperature-corrected quantitative T1, T2, and PD values. Tests were performed between different non-pathologic organ types (liver, spleen, pancreas, and kidney). The receiver operator characteristic (ROC) curve approach was applied to give accuracy of discrimination between the tested quantified temperature-corrected organs. Accuracy was measured by the area under the ROC curve (AUC) with the traditional academic point system: 0.90–0.1 = excellent; 0.80–0.90 = good; 0.70–0.80 = fair; 0.60–0.70 = poor; and 0.50–0.60 = fail. Regression analysis for correlation of temperature-corrected and non-corrected quantitative T1, T2, and PD values of each organ type with post-mortem intervals, and the age and sex of the study population were analyzed using the Pearson product moment correlation. *P* values below 0.05 were assumed to be significant.

## Results

Of 80 forensic corpses, the numbers of histologically confirmed non-pathologic organs were as follows: liver ($n = 26$); spleen ($n = 65$); pancreas ($n = 41$); kidney cortex ($n = 24$), kidney medulla ($n = 24$).

Body core temperatures of 80 corpses ranged from 5 to 34.5 °C (mean temperature 19.4 °C, SD 6.2). MR scanner room temperature was at approx. 24 °C. Table 1 gives linear equations generated from T1/temperature, T2/temperature, and PD/temperature plots for non-pathologic organs. Temperature dependence of quantitative values was observed mainly for T1 values. T2 and PD values were minor influenced by temperature (Fig. 2). Table 2 also gives the mean T1, T2, and PD values and standard deviations assessed for non-pathologic organs. Temperature correction of quantitative

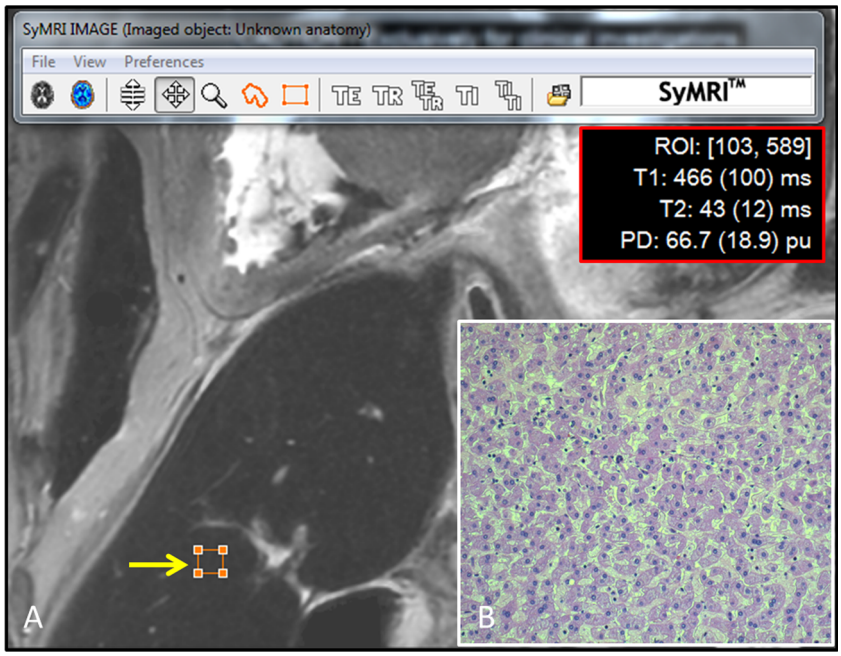


**Fig. 1** *a* Exemplary measurement of quantitative values in synthetically calculated QPMMRI T2w image using the SyMRI Autopsy® tool. In this case, quantitative T1, T2, and PD values of the right liver lobe liver were assessed. After placing a ROI (*yellow arrow*), the respective quantitative values within the ROI are given in a viewport (*red frame upper right*). *b* Histologic examinations were conducted on each measured organ to detect non-pathologic organs. In this case, non-pathologic liver tissue was diagnosed

values resulted in lower standard deviations mainly of the T1 values in all investigated organs.

Figure 3 depicts plots visualizing the mean temperature-corrected quantitative T1, T2, and PD values of non-pathologic organ types. Based on their assessed quantitative T1, T2, and PD values, a significant difference between non-pathologic liver, spleen, pancreas, and kidney was verified by statistical analysis (Table 3). ROC analysis showed that accuracy of discrimination was at least good or excellent in each investigated non-pathologic comparison group (Table 3). Regression analysis revealed no significant correlation of the quantitative values for T1, T2, and PD (of all organ types compared with PMI, sex and age of the deceased (all *P* values >0.05).

## Discussion

The results of the present basic research study indicate that non-pathologic upper abdominal organs such as the liver, pancreas, spleen, and kidneys can be uniquely characterized and discerned based on their T1 and T2 relaxation times and proton density in 1.5 T QPMMRI applications. These findings may provide a basis for promising future applications of simultaneous 1.5 T T1, T2, and PD quantification in post-mortem imaging. QPMMRI may be used to detect and characterize pathologic alterations in upper abdominal organs. Since changes in tissue composition are known to result in changes of relaxation times and proton density, it is likely to hypothesize that basic pathologic alterations such as edema, tumor, inflammation, fibrous or fatty degeneration, and infarction exhibit unique combinations of T1, T2, and PD values [5, 8, 9, 12]. If the quantitative post-mortem value combinations of non-pathologic upper abdominal organs and tissues are known, they may be discerned from the value combinations of pathologic alterations. In clinical in vivo imaging, MR quantification has been demonstrated being feasible to characterize pathologic alterations such as tumor, inflammation, and infarction in various parenchymal tissues and organs [17–22]. However, post-mortem MR imaging is far different from clinical imaging due to varying body temperatures and post-mortem-related tissue changes that influence water

**Table 1** Equations for temperature correction

| | Liver | Spleen | Pancreas | Kidney cortex | Kidney medulla |
|---|---|---|---|---|---|
| T1/temperature | T1 = 3.8 T + 341 | T1 = 3 T + 459 | T1 = 2.02 T + 366 | T1 = 2.9 T + 373 | T1 = 5.3 T + 443 |
| T2/temperature | T2 = 0.1 T + 52 | T2 = 0.08 T + 55 | T2 = 0.01 T + 69 | T2 = 0.2 T + 72 | T2 = −0.07 T + 114 |
| PD/temperature | PD = −0.01 T + 69 | PD = 0.14 T + 69 | PD = 0.1 T + 77 | PD = −0.06 T + 82 | PD = −0.02 T + 70 |

Linear equations generated from relation of quantitative T1, T2, and PD values to body core temperature at the time of MR scanning. Only organs that presented non-pathologic in histologic examinations were included. (T1: T1 relaxation time in milliseconds; T2: T2 relaxation time in milliseconds; T: body core temperature in °C; PD: proton density in % related to pure water (100%))

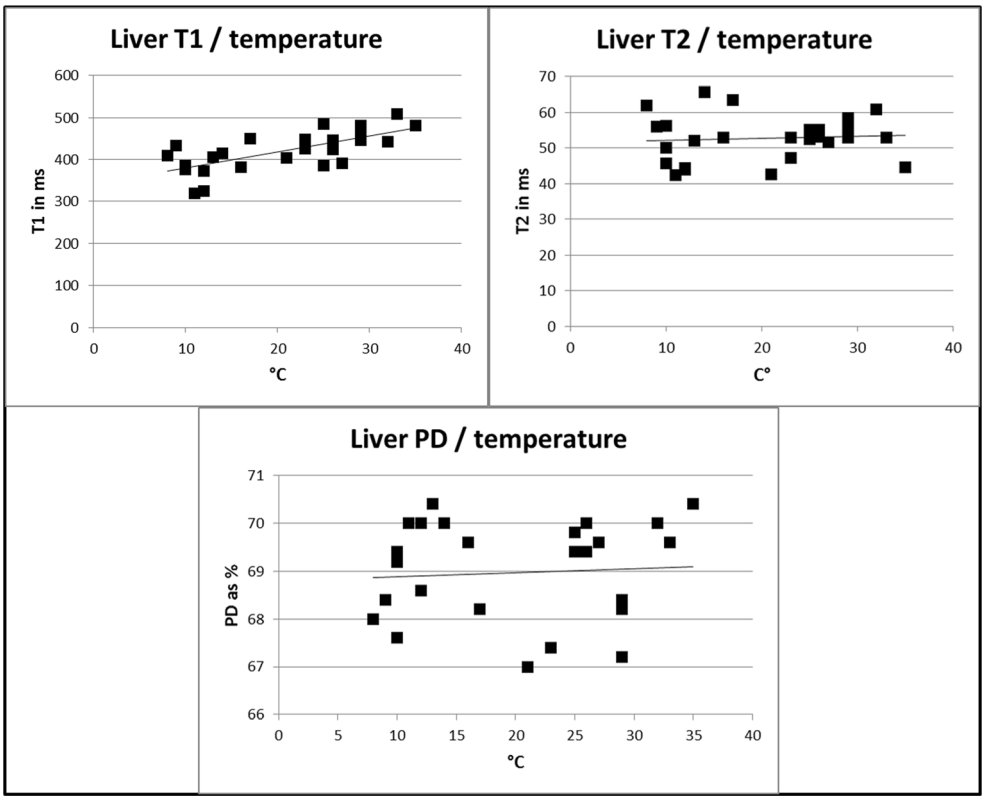


**Fig. 2** Exemplary plots of liver T1 and T2 relaxation times and PD vs. body core temperature at the time of MR scanning. Note that strong temperature dependence is observed for the T1 values

content and pH values of tissues [3–5, 9]. Hence, the actual possibilities of specific pathology determination in abdominal QPMMRI need to be determined yet. In the next step, systematic evaluations of the quantitative T1, T2, and PD values of the manifold relevant specific pathologic alterations of upper abdominal organs such as fatty degeneration in the liver, acute inflammation in the pancreas, or proximal tubular necrosis in the kidney need to be conducted in appropriate case numbers. If the values of specific pathologic alterations differ to the values of non-pathologic organs, 1.5 T QPMMRI may provide an easy to use examination tool in post-mortem imaging enabling the image reader to perform and interpret diagnostic quantitative measurements in the upper abdominal organs. MR quantification has only recently been introduced to post-mortem imaging and this is the first 1.5 T PMMRI study in which the quantitative T1, T2, and PD value combinations of upper abdominal organs were investigated and compared to each other. A previous quantitative 3 T PMMRI study investigated the quantitative T1, T2, and PD values of the liver and spleen with regard to varying body temperatures. In accordance with the present 1.5 T PMMRI study, organs exhibited unique combinations of T1, T2, and PD quantification values [9]. However, the assessed T1 and T2 values differed between the previous 3 T study and the present 1.5 T study. This was an expected finding as it is known that changes in magnetic field strength influence relaxation behaviors of protons in one and the same tissue type leading to different relaxation times [13]. Since both 1.5 and 3 T MR machines are being used in post-

**Table 2** Mean quantification values of non-pathologic organs

| | T1 (SD; CV) Not corrected | T1 (SD; CV) Corrected 37 °C | T2 (SD; CV) Not corrected | T2 (SD; CV) Corrected 37 °C | PD (SD; CV) Not corrected | PD (SD; CV) Corrected 37 °C |
|---|---|---|---|---|---|---|
| Liver ($n$ = 26) | 418.33 (46.7; 0.11) | 485.83 (28.3; 0.05) | 52.68 (6.4; 0.12) | 53.52 (6.1; 0.11) | 68.85 (5.3; 0.08) | 68.68 (4.3; 0.06) |
| Spleen ($n$ = 65) | 517.92 (47.3; 0.1) | 570.90 (29.8; 0.05) | 56.98 (7.9; 0.13) | 57.15 (6.5; 0.11) | 71.77 (4.6; 0.06) | 74.06 (4.1; 0.06) |
| Pancreas ($n$ = 41) | 404.71 (33.6; 0.08) | 438.89 (26.7; 0.06) | 68.78 (7.6; 0.11) | 68.72 (7.3; 0.1) | 78.96 (7.6; 0.09) | 80.06 (6.7; 0.08) |
| Kidney cortex ($n$ = 24) | 432.64 (35.1; 0.08) | 482.25 (29; 0.06) | 76.4 (7.3; 0.09) | 79.50 (6.7; 0.08) | 80.48 (5.8; 0.07) | 79.47 (5.1; 0.06) |
| Kidney medulla ($n$ = 24) | 549.56 (42.7; 0.07) | 637.67 (28.7; 0.04) | 112.15 (7.8; 0.07) | 110.97 (7.8; 0.07) | 69.50 (5.5; 0.08) | 69.17 (5.5; 0.08) |

Mean quantification values (T1 and T2 in milliseconds; PD in %; obtained from nine measurements), standard deviations (SD), and coefficients of variations (CV) of histologically confirmed non-pathologic upper abdominal organs in 80 forensic cases. Data are presented with and without temperature correction to 37 °C

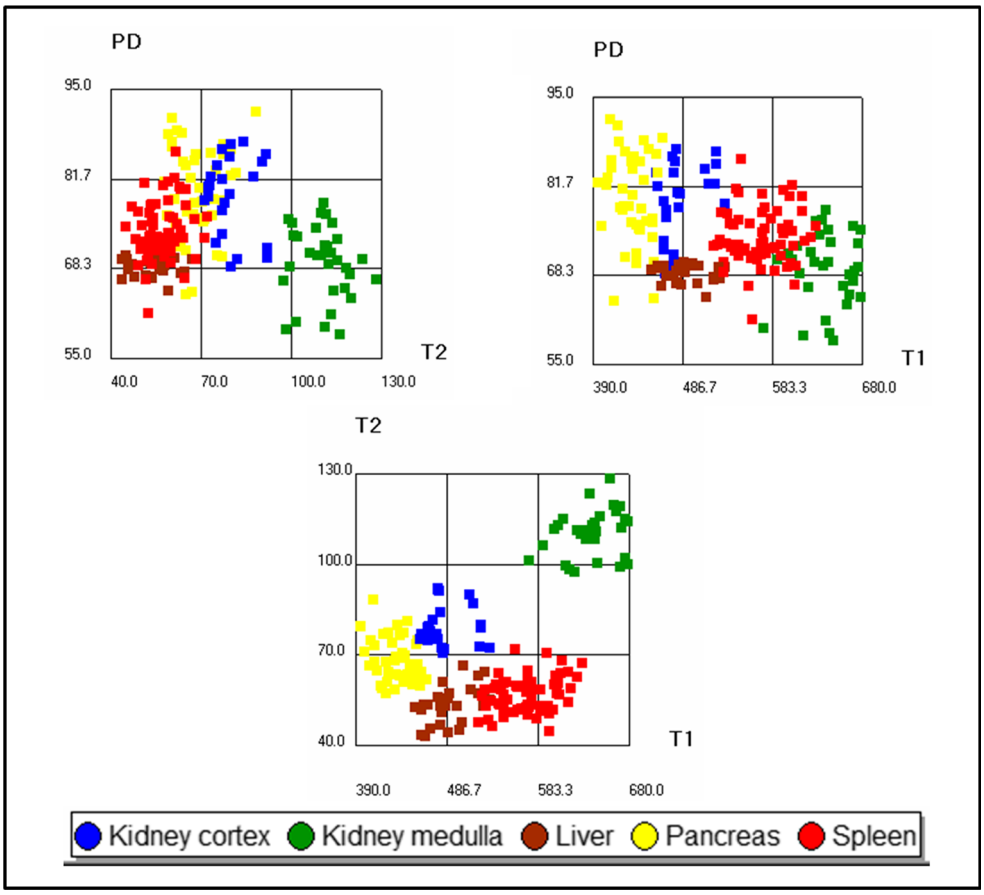


**Fig. 3** Plots of the mean temperature-corrected (37 °C) T1, T2, and PD values of non-pathologic organs. Each *square* represents a single organ. Three defined views (T2/T1 view, PD/T1 view, and PD/T2 view) are shown. Best visual differentiation between organ types can be observed in the T2/T1 view

mortem imaging, both 1.5 and 3 T quantitative values need to be assessed if QPMMRI is to be used for practical post-mortem casework in the future. When using 3 T machines in post-mortem quantitative MR, increased specific absorption rate (SAR) due to higher magnetic field strength may be hypothesized to impair the method due to significant heating of the corpse. In the present study, SAR was at 2 W/kg. The energy required for 1 l of water to increase 1° is 4200 J,

**Table 3** ANOVA testing and ROC analysis

| | T1 corrected to 37 °C | T2 corrected to 37 °C | PD corrected to 37 °C | ROC-AUC/ accuracy |
|---|---|---|---|---|
| Liver-pancreas | <0.05 | <0.001 | <0.001 | 0.94/excellent |
| Liver-spleen | <0.05 | 0.48 | <0.05 | 0.87/good |
| Liver-kidney cortex | 0.63 | <0.001 | <0.05 | 0.85/good |
| Liver-kidney medulla | <0.001 | <0.001 | 0.06 | 0.91/excellent |
| Pancreas-spleen | <0.001 | <0.05 | 0.12 | 0.92/excellent |
| Pancreas-kidney cortex | <0.05 | <0.05 | 0.36 | 0.83/good |
| Pancreas-kidney medulla | <0.001 | <0.001 | <0.05 | 0.95/excellent |
| Spleen-kidney cortex | <0.001 | <0.05 | <0.05 | 0.90/excellent |
| Spleen-kidney medulla | <0.05 | <0.001 | 0.32 | 0.89/good |
| Kidney cortex-kidney medulla | 0.003 | <0.001 | 0.06 | 0.88/good |

Results of one-way ANOVAs with post hoc analysis for comparison of temperature-corrected quantitative T1 (ms), T2 (ms), and PD (%) values. Tests were performed between non-pathologic organ types separately for T1, T2, and PD variables. Bonferroni correction was applied: significant $P$ values <0.004. There is at least one significantly different T1, T2, or PD quantification value in each of the tested groups. A significant difference between all tested organs can be determined. The table also gives the area under the ROC curve (ROC-AUC) for accuracy of discrimination, which was at least good in all tested groups

resulting in 1° in 35 min scan time. The MR scanner room temperature was at approx. 24 °C, which could have increased the temperature further, but this was to be expected mostly on the outer layer of the corpse. Given the abovementioned numbers, it is rather unlikely that the temperature would increase more than 2 °C during the entire acquisition. Hence, an increase of more than 2 °C during MR scan procedure was not observed in any of the scanned 80 cases.

An advantage of MR quantification is that quantitative values such as relaxation times and proton density are not vendor specific and exhibit the same value ranges when assessed with different MR machines [5, 9, 14]. Hence, Shiotani et al. measured T1 and T2 relaxation times of liver tissue in a post-mortem 1.5 T MR application that were in the range of the assessed liver values of the present study [6]. A disadvantage of post-mortem MR quantification is the temperature dependence of relaxation times. In accordance with the results from Shiotani et al., changes in body temperature influenced liver T1 and T2 values in the present study [6]. Moreover, behavior of quantitative T1, T2, and PD values related to body core temperature in all investigated upper abdominal organs was similar to previous post-mortem quantitative MRI 1.5 T brain and heart studies in which T1 values were increasing with rising temperature while T2 and PD values were only minor influenced [8, 9, 11, 12]. These findings stress the necessity of temperature corrections in QPMMRI [9]. The equations established from temperature/quantitative value plots in the present study may be used for temperature correction of quantitative values in the investigated upper abdominal organs for 1.5 T applications. In forensic imaging practice, usually, rectal temperature is taken to assess body core temperature [23]. However, in their forensic imaging practice, the authors noticed variations of 1 to 2 °C between assessed rectal and deep esophageal body core temperatures. Therefore, in the present study, deep esophageal temperature measurements were favored to rectal measurements since the distance of the esophageal probe tip to adjacent upper abdominal organs was significantly shorter than the distance from the rectum to upper abdominal organs. Hence, the measured body core temperature was expected to reflect upper organ temperatures more accurately.

The isotropic nature of the assessed quantitative T1, T2, and PD values may also provide a basis for promising future software applications in QPMMRI. T1, T2, and PD quantification values may be used to develop computer-aided diagnosis software for pathology detection and interpretation. Quantification data also offer the possibility of MR image plane reconstruction and volume rendering on radiological workstations, which would further improve the diagnostic ability of QPMMRI [24–28]. In the field of forensic imaging, quantitative MRI may not only be restricted to post-mortem application but also be a useful adjunct to clinical forensic cases of living persons. Previous studies from Petrovic et al. and Baron et al. indicated that quantitative MRI may be used for age estimation of hematoma or fractures in clinical forensic patients [29, 30].

The present study has noteworthy limitations:

> Quantitative measurements were conducted by only one observer which did not allow for analysis of reproducibility of measurements.

In general, QPMMRI is only feasible in cases without relevant putrefaction. In the present study, quantitative values of measured organs were not influenced by the post-mortem interval. The maximum PMI of cases was 2 days and cases did not exhibit relevant putrefaction. It is likely to hypothesize that changes of tissue composition due to putrefaction would inevitably cause changes of quantitative T1, T2, and PD values in rather large ranges.

## Conclusions

Temperature-corrected 1.5 T QPMMRI based on T1, T2, and PD values is feasible for characterization and differentiation of the non-pathologic liver, spleen, pancreas, and kidney. The results may provide a base for future specific pathology diagnosis of upper abdominal organs in post-mortem imaging.

**Acknowledgements** We would like to express our gratitude to our team of forensic pathologists and forensic technicians for their support with case handling.

**Compliance with ethical standards** PMMRI examinations and usage of the imaging data were approved by the local ethics committee.

## References

1. Patriquin L, Kassarjian A, Barish M et al (2001) Postmortem whole-body magnetic resonance imaging as an adjunct to autopsy: preliminary clinical experience. J Magn Reson Imaging 13(2):277–287
2. Thali MJ, Yen K, Schweitzer W et al (2003) Virtopsy, a new imaging horizon in forensic pathology: virtual autopsy by postmortem multislice computed tomography (MSCT) and magnetic resonance imaging (MRI)—a feasibility study. J Forensic Sci 48(2):386–403
3. Ruder TD, Thali MJ, Hatch GM (2014) Essentials of forensic post-mortem MR imaging in adults. Br J Radiol 87(1036):20130567
4. Jackowski C, Schwendener N, Grabherr S, Persson A (2013) Postmortem cardiac 3T magnetic resonance imaging: visualizing the sudden cardiac death? J Am Coll Cardiol 62(7):617–629
5. Jackowski C, Warntjes M, Kihlberg J, Berge J, Thali M, Persson A (2011) Quantitative MRI in isotropic spatial resolution for forensic soft tissue documentation. Why and how? J Forensic Sci 56(1): 208–215
6. Shiotani S, Kobayashi T, Hayakawa H, Homma K, Sakahara H (2015) Hepatic relaxation times from postmortem MR imaging of adult humans. Magn Reson Med Sci 15(3):281–287

7. Tashiro K, Shiotani S, Kobayashi T et al (2015) Cerebral relaxation times from postmortem MR imaging of adults. Magn Reson Med Sci 14(1):51–56
8. Zech WD, Schwendener N, Persson A, Warntjes M, Jackowski C (2015) Postmortem MR quantification of the heart for characterization and differentiation of ischemic myocardial lesions. Eur Radiol 25(7):2067–2073
9. Zech WD, Schwendener N, Persson A, Warntjes M, Jackowski C (2015) Temperature dependence of postmortem MR quantification for soft tissue discrimination and sequence optimization. Eur Radiol 25(8):2381–2389
10. Zech WD, Schwendener N, Persson A et al (2015) Postmortem quantitative 1.5 T MRI for the differentiation and characterization of serous fluids, blood, CSF and putrefied CSF. Int J Legal Med 129(5):1127–1136
11. Zech WD, Hottinger A, Schwendener N et al (2016) Quantitative post-mortem 1.5T neuro MRI for assessment of regular anatomical brain structures. Int J Legal Med 130(4):1071–1080
12. Schwendener N, Jackowski C, Persson A, et al (2016) Detection and differentiation of early acute and following age stages of myocardial infarction with quantitative post-mortem cardiac 1.5T MR. Forensic Sci Int. doi:10.1016/j.forsciint.2016.10.014.
13. Haacke ME, Brown RW, Thompson MR, Venkatesh N (1999) Magnetic resonance imaging-physical principles and sequence design. John Wiley & Sons, New York, NY
14. Warntjes JB, Leinhard OD, West J, Lundberg P (2008) Rapid magnetic resonance quantification on the brain: optimization for clinical usage. Magn Reson Med 60:320–329
15. SyntheticMR products website (2016) Available via: http://www.syntheticmr.com. Accessed 22 Sept 2016
16. Committee of Ministers to member states (2000) Recommendation no. R (99) 3 on the harmonization of medico-legal autopsy rules. Forensic Sci Int 111(1–3):5–58
17. Verhaert D, Thavendiranathan P, Giri S et al (2011) Direct T2 quantification of myocardial edema in acute ischemic injury. JACC Cardiovasc Imaging 4:269–278
18. Park CH, Choi EY, Greiser A et al (2013) Diagnosis of acute global myocarditis using cardiac MRI with quantitative t1 and t2 mapping: case report and literature review. Korean J Radiol 14(5):727–732
19. Lescher S, Jurcoane A, Veit A et al (2015) Quantitative T1 and T2 mapping in recurrent glioblastomas under bevacizumab: earlier detection of tumor progression compared to conventional MRI. Neuroradiology 57(1):11–20
20. Wang A, Pedoia V, Su F et al (2016) MR T1ρ and T2 of meniscus after acute anterior cruciate ligament injuries. Osteoarthr Cartil 24(4):631–639
21. Cassinotto C, Feldis M, Vergniol J et al (2015) MR relaxometry in chronic liver diseases: comparison of T1 mapping, T2 mapping, and diffusion-weighted imaging for assessing cirrhosis diagnosis and severity. Eur J Radiol 84(8):1459–1465
22. Stollfuss JC, Becker K, Sendler A et al (2006) Rectal carcinoma: high-spatial-resolution MR imaging and T2 quantification in rectal cancer specimens. Radiology 241(1):132–141
23. Ruder TD, Hatch GM, Siegenthaler L et al (2012) The influence of body temperature on image contrast in post mortem MRI. Eur J Radiol 81(6):1366–1370
24. Lundström C, Persson A, Ross S et al (2012) State-of-the-art of visualization in post-mortem imaging. APMIS 120(4):316–326
25. Vågberg M, Lindqvist T, Ambarki K et al (2013) Automated determination of brain parenchymal fraction in multiple sclerosis. AJNR 34(3):498–504
26. Wu Y, Yang R, Jia S, Li Z, Zhou Z, Lou T (2014) Computer-aided diagnosis of early knee osteoarthritis based on MRI T2 mapping. Biomed Mater Eng 24(6):3379–3388
27. Giannini V, Mazzetti S, Vignati A et al (2015) A fully automatic computer aided diagnosis system for peripheral zone prostate cancer detection using multi-parametric magnetic resonance imaging. Comput Med Imaging Graph 46(Pt 2):219–226
28. Gallego-Ortiz C, Martel AL (2015) Improving the accuracy of computer-aided diagnosis for breast MR imaging by differentiating between mass and nonmass lesions. Radiology 278(3):679–688
29. Petrovic A, Krauskopf A, Hassler E, Stollberger R, Scheurer E (2016) Time related changes of T1, T2, and T2* of human blood in vitro. Forensic Sci Int 262:11–17
30. Baron K, Neumayer B, Widek T et al (2016) Quantitative MR imaging in fracture dating—initial results. Forensic Sci Int 261: 61–69